CONDENSED MATTER PHYSICS

Detection of thermodynamic "valley noise" in monolayer semiconductors: Access to intrinsic valley relaxation time scales

M. Goryca[1,2], N. P. Wilson[3], P. Dey[1], X. Xu[3], S. A. Crooker[1]*

Together with charge and spin, many novel two-dimensional materials also permit information to be encoded in an electron's valley degree of freedom—that is, in particular momentum states in the material's Brillouin zone. With a view toward valley-based (opto)electronic technologies, the intrinsic time scales of valley scattering are therefore of fundamental interest. Here, we demonstrate an entirely noise-based approach for exploring valley dynamics in monolayer transition-metal dichalcogenide semiconductors. Exploiting their valley-specific optical selection rules, we use optical Faraday rotation to passively detect the thermodynamic fluctuations of valley polarization in a Fermi sea of resident carriers. This spontaneous "valley noise" reveals narrow Lorentzian line shapes and, therefore, long exponentially-decaying intrinsic valley relaxation. Moreover, the noise signatures validate both the relaxation times and the spectral dependence of conventional (perturbative) pump-probe measurements. These results provide a viable route toward quantitative measurements of intrinsic valley dynamics, free from any external perturbation, pumping, or excitation.

INTRODUCTION

The development of novel two-dimensional (2D) materials such as graphene, bilayer graphene, and monolayer transition metal dichalcogenide (TMD) semiconductors has rejuvenated long-standing interests (*1*, *2*) in harnessing valley degrees of freedom (*3*–*10*). Encoding information in an electron's momentum state (i.e., by which valley in the material's Brillouin zone the electron occupies) forms the conceptual basis of the burgeoning field of "valleytronics." In particular, the family of monolayer TMDs such as MoS_2 and WSe_2 has focused attention on valley physics because they provide a facile means of addressing specific valleys in momentum space using light: Owing to strong spin-orbit coupling and lack of crystalline symmetry, monolayer TMDs have valley-specific optical selection rules (*11*–*14*), wherein right and left circularly polarized light couples selectively to transitions in the distinct K and K' valleys of their hexagonal Brillouin zone. Valley-polarized electrons, holes, and excitons can therefore be readily injected and detected optically, in marked contrast to most conventional semiconductors.

For any foreseeable valley-based information processing scheme, the intrinsic time scales of valley scattering and relaxation are of obvious critical importance. Recent optical pump-probe studies have shown that while valley-polarized electron-hole pairs (excitons) scatter very quickly on picosecond time scales (*15*–*21*), the valley relaxation of resident carriers in electron- or hole-doped monolayer TMD semiconductors can be orders of magnitude longer (*22*–*27*), even in the range of microseconds for holes at low temperatures (*28*, *29*). However, while very encouraging, all these pump-probe measurements are necessarily perturbative in nature. This is because optical pumping injects nonequilibrium electrons and holes that scatter, dissipate energy, and interact, thereby perturbing the resident carriers' valley polarization away from thermal equilibrium via processes not yet well understood. Moreover, optical pumping of both majority and minority carriers can create optically inactive "dark" excitons and trions (*30*–*33*), whose presence, if sufficiently long lived, could, in principle, mask detection of carrier valley relaxation, as recently suggested (*34*, *35*). An alternative means of accessing the truly intrinsic valley relaxation of resident carriers in monolayer TMDs, free from perturbative or dark exciton effects, is therefore highly desired.

Fortunately, the fundamental relationship between a system's dynamic linear response (i.e., susceptibility) and its intrinsic fluctuations, as articulated by the fluctuation-dissipation theorem (*36*), suggests an alternative approach. Rather than perturb the valley polarization and measure its dissipative response, one could instead attempt to detect the spontaneous valley fluctuations that necessarily must exist even in thermal equilibrium. If measurable, this thermodynamic "valley noise" encodes the truly intrinsic relaxation time scales. Here, we demonstrate that stochastic valley noise is measurable in monolayer TMD semiconductors using optical Faraday rotation (FR) and, furthermore, can be used as a powerful and unambiguous probe of the intrinsic valley dynamics in a Fermi sea of resident carriers, free from any external perturbation, pumping, or excitation.

RESULTS

Figure 1A depicts the sample, which is an exfoliated WSe_2 monolayer sandwiched between 25-nm-thick slabs of hexagonal boron nitride (hBN). To electrostatically gate the resident carrier density in the WSe_2, part of the monolayer contacts a gold pad, and a separately contacted thin graphite layer serves as a top gate. The sample is assembled on a transparent silica substrate and covered with a final hBN layer for mechanical stability. Unless otherwise stated, we performed all measurements in the lightly hole-doped regime using a fixed gate voltage V_g = +2 V (giving an estimated hole density of $1.2 \times 10^{12}/cm^2$). All results presented here were also qualitatively confirmed on a second sample, with nominally the same structure.

Figure 1B shows a simple band diagram of a hole-doped WSe_2 monolayer, along with the optical selection rules in the K and K' valleys that couple to right and left circularly polarized (σ^+ and σ^-) light, respectively. The absorption of $\sigma^{\pm}$ light depends sensitively on

[1]National High Magnetic Field Laboratory, Los Alamos, NM 87545, USA. [2]Institute of Experimental Physics, Faculty of Physics, University of Warsaw, Warsaw, Poland. [3]Department of Physics, University of Washington, Seattle, WA 98195, USA. *Corresponding author. Email: crooker@lanl.gov

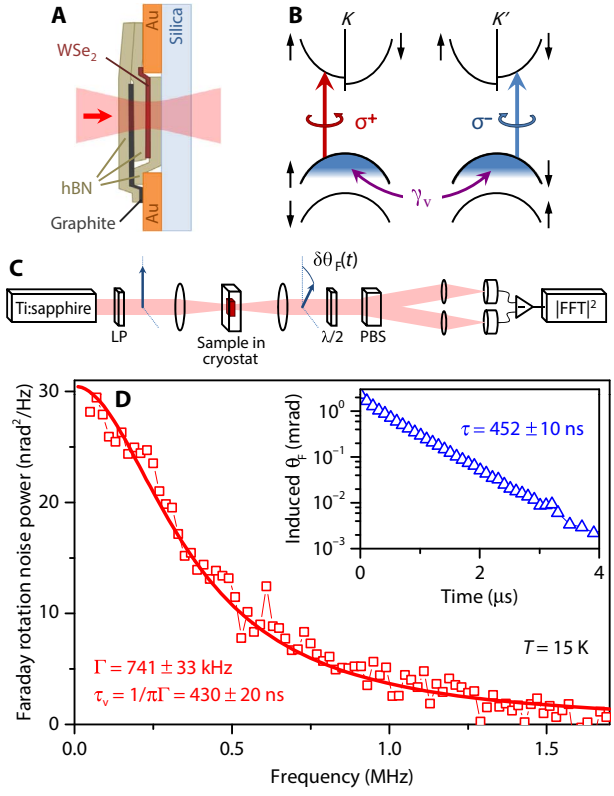

Fig. 1. Sample, experimental setup, and valley noise spectrum of resident holes in monolayer WSe_2. (**A**) Sample: A single WSe_2 monolayer is sandwiched between hBN layers and electrically gated. (**B**) Band structure and $\sigma^{\pm}$ optical transitions of hole-doped monolayer WSe_2. Even in thermal equilibrium, resident holes spontaneously scatter between *K* and *K*′ valleys, giving a randomly fluctuating valley polarization noise. (**C**) To detect valley noise, a CW probe laser is linearly polarized and focused through the sample. Thermodynamic valley fluctuations impart FR fluctuations $\delta\theta_F(t)$ on the probe laser, which are detected using balanced photodiodes. LP, linear polarizer; PBS, polarizing beam splitter; FFT, fast Fourier transform. (**D**) The valley noise power spectrum (squares) of resident holes in monolayer WSe_2. Its Lorentzian line shape (solid line) with full width Γ indicates an exponentially decaying valley correlation with relaxation time scale $\tau_v = 1/\pi\Gamma = 430 \pm 20$ ns. Inset: Valley relaxation measured separately in a perturbative pump-probe experiment.

the densities of resident holes, $p^{\pm}$ (especially at energies *E* near the positively charged exciton resonance, as discussed in detail later). Associated with the $\sigma^{\pm}$ absorptions are the dispersive indices of refraction, $n^{\pm}(E)$. The difference between these indices is measured by optical FR, θ_F. By definition, $\theta_F(E) \propto n^+(E) - n^-(E)$, which, in turn, is inherently sensitive to the holes' valley polarization, $p^+ - p^-$. For these reasons, θ_F (and its close relative, Kerr rotation θ_K) is often used to probe the nonequilibrium valley polarizations that are induced in conventional pump-probe studies (*24*–*29*, *35*).

In thermal equilibrium (and in zero magnetic field), the time-averaged valley polarization of the hole Fermi sea is strictly zero: $\langle p^+ - p^- \rangle = 0$, $\langle n^+ - n^- \rangle = 0$, and therefore $\langle \theta_F(t) \rangle = 0$. However, thermodynamic fluctuations always exist, and holes in the *K* valley can spontaneously scatter to the *K*′ valley (or vice versa) with intrinsic rate $\gamma_v = 1/\tau_v$, leading to a small valley polarization that fluctuates randomly in time about zero. This valley noise can, in principle, be detected as a fluctuating FR $\delta\theta_F(t)$. The temporal correlation function of this valley noise, $S(t) = \langle \delta\theta_F(0)\delta\theta_F(t) \rangle$, will be determined by the intrinsic time scales of valley scattering and relaxation in the TMD monolayer (*36*). This overall approach is analogous to studies of optical spin noise spectroscopy in atomic alkali vapors (*37*, *38*) and certain conventional semiconductors (*39*–*41*) in which $\sigma^{\pm}$ light couples to specific spin (but not valley) states due to the presence of spin-orbit coupling.

The experiment is shown in Fig. 1C. The sample is mounted on the cold finger of a small optical cryostat. A continuous-wave (CW) probe laser is linearly polarized and focused to a small (3 to 10 μm in diameter) spot on the sample. We typically tune the laser well below the charged exciton (X^+) transition energy and use small (tens of microwatts) power to avoid any interband excitation of the monolayer. Stochastic valley noise imparts small FR fluctuations $\delta\theta_F(t)$ on the transmitted probe laser, which are detected with sensitive balanced photodiodes. This fluctuating signal is amplified and digitized, and its power spectrum is computed and signal averaged in real time using fast Fourier transform methods.

Figure 1D shows the main result, which is the direct observation of thermodynamic valley fluctuations from resident carriers (holes) in a single monolayer of the archetypal TMD semiconductor WSe_2. The probe laser is tuned to 1.694 eV, which is ~10 meV below the X^+ resonance and, therefore, in the forbidden bandgap of the WSe_2. The detected valley noise is very small, amounting to only a few tens of square nanoradians per hertz of FR noise power, which is typically ~0.1% of the background (uncorrelated) noise power that is due to fundamental photon shot noise and amplifier noise (see fig. S1). To subtract off this constant background noise, what Fig. 1D shows is actually the difference between averaged noise spectra acquired on the WSe_2 flake and averaged noise spectra acquired just off the flake where the probe beam passes only through the hBN layer and the substrate. The valley noise spectrum shown in Fig. 1D required tens of hours to obtain, with repeated repositioning of the probe beam off and on the sample to compensate for small drifts of laser power.

The resulting noise spectrum is peaked at zero frequency and has a Lorentzian line shape, with full width at half maximum $\Gamma = 741 \pm 33$ kHz. Because the power spectrum of $\delta\theta_F(t)$ is equivalent [per the Wiener-Khinchin theorem (*36*)] to the Fourier transform of the temporal correlation function $S(t) = \langle \delta\theta_F(0)\delta\theta_F(t) \rangle$, a Lorentzian noise spectrum indicates that $S(t)$ decays exponentially, with a single time scale. This time scale is precisely the intrinsic valley relaxation time τ_v, which is related to the inverse width of the noise power spectrum: $\tau_v = 1/(\pi\Gamma)$. Therefore, the noise spectrum in Fig. 1D reveals a very long valley relaxation time $\tau_v = 430 \pm 20$ ns for resident holes in this WSe_2 monolayer (at 15 K and at this hole density). In this manner, the intrinsic time scales of valley relaxation in monolayer TMD semiconductors are revealed simply by passively "listening" to the thermodynamic valley fluctuations alone and without ever perturbing, pumping, or exciting the Fermi sea of resident holes away from equilibrium.

Such a long intrinsic τ_v is consistent with very recent reports of extremely long valley relaxation of resident holes in WSe_2 (*28*, *29*), which result from strong spin-valley locking in the valence bands of monolayer TMDs (*12*). As depicted in Fig. 1B, for a hole to scatter/relax between the uppermost valence bands in the *K* and *K*′ valleys, it must not only substantially change its momentum but also simultaneously flip its spin. The low probability for this to occur means that measured relaxation time scales can be long, of the order of microseconds at low temperatures.

We use the noise-based methodology to resolve lingering concerns about the validity of conventional (i.e., perturbative) pump-probe studies of doped TMD monolayers (*23*–*29*)—namely, whether long-lived dark excitons, dark trions, or other perturbations can masquerade as

slow valley relaxation of resident carriers. We directly compare τ_v obtained from the valley noise to the decay time measured independently by optical pump-probe experiments. Using pulsed lasers, we perform a time-resolved FR (TRFR) study of the same WSe_2 monolayer (at the same T and V_g), using methods described previously (*29*). Here, 1.922-eV pump pulses inject valley-polarized electrons and holes into the WSe_2, which scatter, relax, and recombine, eventually perturbing the hole Fermi sea and generating a nonequilibrium valley polarization. The dissipative relaxation of the hole polarization back to equilibrium is monitored by the FR imparted on time-delayed 1.694-eV probe pulses. The nearly monoexponential decay of the induced valley polarization is shown in the inset of Fig. 1D. The decay time is 450 ± 10 ns, which is in close agreement with the valley correlation (relaxation) time τ_v inferred from passive detection of the equilibrium fluctuations alone. It is worth noting that, in contrast to many previous experiments (*24*–*29*, *35*), the decay does not show any fast (<10 ns) components, likely due to the high quality of the sample and hBN encapsulation. Because the valley noise detection is entirely passive and does not involve any optical pumping or excitation (as verified in more detail below), τ_v cannot be due to the presence of optically inactive dark excitons or trions. The very close agreement between the valley decay time measured by conventional TRFR and τ_v measured from valley noise therefore proves that long-lived TRFR signals observed here also arise principally from the valley polarization of resident carriers and do not arise from dark states or other long-lived excitations.

Figure 2 shows the temperature dependence of the valley relaxation time τ_v determined by noise experiments, along with a comparison to τ_v measured by conventional TRFR methods. Figure 2A shows normalized valley noise spectra obtained at T = 15, 20, 25, and 29 K. All are well described by Lorentzian line shapes, with Γ ($=1/\pi\tau_v$) increasing significantly to 4.5 MHz at 29 K, indicating a reduction of τ_v. Separately, conventional TRFR measurements of valley dynamics (Fig. 2B) also show faster decays at higher temperature. Figure 2C compares τ_v as measured by the two methods, again showing very close agreement and further establishing that the long-lived TRFR signals arise from intrinsic valley polarization of resident carriers and are not dark exciton effects. The marked temperature dependence of valley relaxation in TMD monolayers was also observed in (*24*, *25*, *28*, *29*).

We obtained the valley noise spectra in Fig. 2 using a different and much more efficient method of background subtraction, which was found during the course of these studies: Rather than acquire background noise spectra by repositioning the probe laser off the monolayer WSe_2 flake (as in Fig. 1D), backgrounds are instead acquired in the presence of an in-plane magnetic field B_x. Both noise and TRFR studies reveal that applied $B_x > 0.3$ T suppresses τ_v by nearly an order of magnitude in these encapsulated WSe_2 monolayers (see figs. S2 and S3). Thus, the resulting valley noise spectrum is comparatively small and nearly flat at low frequencies and, therefore, can be used as a reliable and very convenient background against which to compare the much narrower and larger zero-field valley noise that is the focus of these studies (experimentally, applying B_x is less time-consuming than repeatedly repositioning the probe laser on and off the WSe_2 flake). Figure 2D shows excellent agreement between the valley noise spectra obtained by the two background subtraction methods. We note that B_x-dependent valley relaxation is not actually expected in hole-doped TMD monolayers due to the large spin-orbit splitting of the valence bands (which, in principle, acts as a large stabilizing out-of-plane magnetic field), and earlier pump-probe studies of hole-doped WSe_2 monolayers showed very little dependence on B_x (*25*, *29*). As discussed in fig. S2, we speculate that the very different encapsulation and gating scheme we use (full hBN encapsulation here versus no encapsulation in earlier works) and associated defects and local strain environment may play important roles. Although a full understanding of field-dependent effects is not yet achieved and lies outside the scope of this work, we can nonetheless exploit this behavior to efficiently subtract off the background to obtain the valley noise. This allows much more detailed studies of valley fluctuations from resident carriers, for example, as a function of probe laser intensity and photon energy, as discussed below.

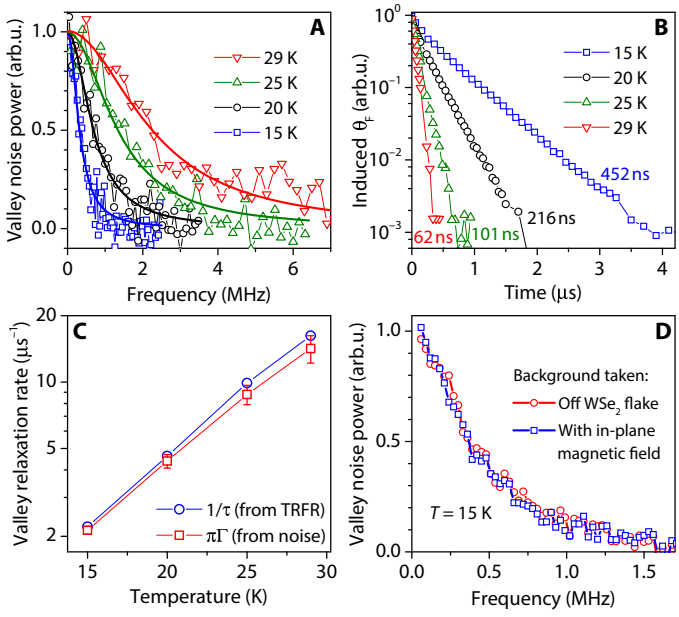

Fig. 2. Comparing the valley noise measurements with perturbative pump-probe experiments. (**A**) Valley noise spectra of hole-doped WSe_2 at different temperatures (solid lines are Lorentzian fits). arb.u., arbitrary units. (**B**) Hole valley relaxation measured separately by TRFR. (**C**) Temperature dependence of valley relaxation rate extracted from the valley noise ($1/\tau_v = \pi\Gamma$; red) and relaxation rate measured by TRFR (blue) showing very close agreement. (**D**) Valley noise spectra acquired using two different background subtraction methods: on/off the WSe_2 (red) and absence/presence of in-plane magnetic field B_x (blue). See also fig. S3 for a more detailed field and temperature dependence.

To confirm that the probe laser in the noise experiments does behave as a passive detector of intrinsic valley fluctuations (and is not inadvertently perturbing the sample by, for example, exciting real carriers), we investigate the dependence of the measured noise on the parameters of the probe laser. Figure 3A shows that the total frequency-integrated noise power scales inversely with the cross-sectional area of the probe laser spot on the sample, which we vary by moving the sample in an out of the beam focus. An inverse-area dependence is a hallmark of optically detected noise signals, well established from earlier studies of spin noise in atomic vapors (*37*) and semiconductors (*40*). We briefly summarize the reason for this dependence as follows: Consider the ensemble of $N = pA$ holes within the probe laser spot, where p is the hole density and A is the spot area. The number of holes that randomly fluctuate between the K and K' valleys is proportional to $\sqrt{N}$. Therefore, the fluctuations of holes' valley polarization (which is probed by FR) scale with $\sqrt{N}/N = 1/\sqrt{N} = 1/\sqrt{pA}$, which increases when A shrinks and N becomes small. At the smallest spot size, we estimate that the measured noise arises from valley fluctuations of the order of ±50 holes (assuming that only holes within k_BT of the Fermi energy

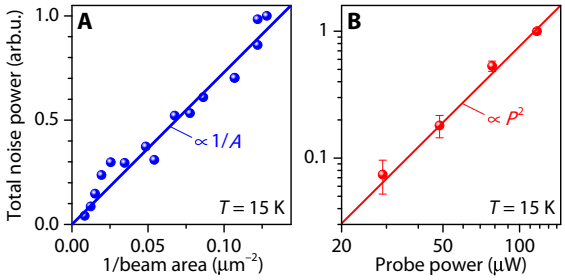

Fig. 3. Dependence of the measured noise on probe parameters. (**A**) The total (frequency-integrated) valley noise power scales as the inverse of the cross-sectional area *A* of the probe laser spot on the sample, as expected for optically detected noise measurements. (**B**) The total valley noise scales quadratically with the power *P* of the probe laser, again as expected for noise studies.

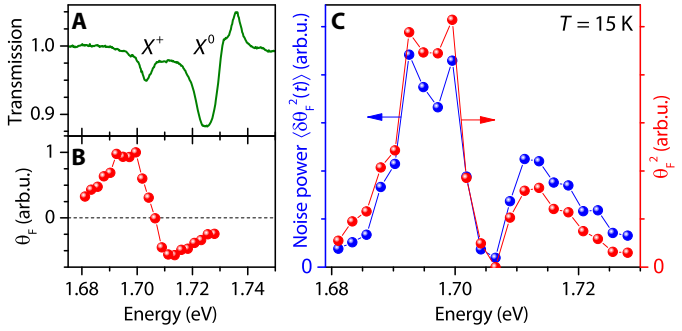

Fig. 4. Dependence of the hole valley noise on the probe photon energy. (**A**) Optical transmission spectrum of the lightly hole-doped WSe_2 monolayer (V_g = +2 V) showing neutral (X^0) and positively charged exciton (X^+) resonances. (**B**) Energy-dependent FR spectrum $\theta_F(E)$ induced by an intentional (optically pumped) valley polarization of the resident holes (see text). $\theta_F(E)$ is antisymmetric and centered on X^+, as expected. (**C**) Spectral dependence of the total valley noise power, $\langle\delta\theta_F^2(t)\rangle$ (blue points). The red points show the square of $\theta_F(E)$ from (B), showing close agreement.

can scatter, where k_B is the Boltzmann constant). Separately, Fig. 3B shows the dependence of the measured noise on the probe laser power. For a given fluctuation in the sample, doubling the probe power should trivially double the fluctuating voltage generated by the photodiodes, quadrupling the measured noise power (in units of volts squared of total detected noise), which is observed. Any deviations from the inverse-area dependence or the quadratic power dependence could indicate that the probe itself is pumping or perturbing the sample.

We also investigate the dependence of the hole valley noise on the probe photon energy *E* and show that the noise is largest when the probe laser is tuned near to—but not on—the X^+-charged exciton transition. Figure 4A shows the transmission spectrum of the lightly hole-doped WSe_2 monolayer. The X^+ absorption appears as a very narrow (4.7 meV wide) resonance at 1.703 eV, which is ~22 meV below the neutral exciton resonance (X^0 is still visible at this small hole density; see fig. S4 for gate-dependent absorption spectra). For reference, we first show in Fig. 4B the result of a conventional CW pump-probe FR experiment in which a weak circularly polarized CW pump laser (at 1.96 eV) generates a steady-state nonequilibrium valley polarization in the hole Fermi sea, while the induced FR spectrum $\theta_F(E)$ is concurrently measured by a tunable CW probe laser. Note that $\theta_F(E)$ shows a clear antisymmetric (dispersive) resonance line shape, in accordance with the fact that $\theta_F(E)$ depends on the dispersive indices of refraction, $n^+(E) - n^-(E)$, which, in turn, depend on the resident hole polarization. The spectral width of the $\theta_F(E)$ resonance appears greater than the absorption width, in agreement with the Kramers-Kronig relations between the real (dispersive) and imaginary (absorptive) parts of the complex dielectric function. Importantly, $\theta_F(E)$ is centered on the X^+ absorption resonance, in agreement with the expectation that it is the charged exciton transitions (not neutral excitons) that depend explicitly on the presence of resident carriers—i.e., by definition, the σ^+/σ^--polarized X^+ transition can only have oscillator strength if there are preexisting (resident) holes in the K'/K valleys, respectively.

Hence, we may therefore anticipate that a polarization of the hole Fermi sea due to thermodynamic valley fluctuations will generate a similar spectral response that is centered on the X^+ transition and that the spectrum of the valley noise power $\langle\delta\theta_F^2(t)\rangle$ will resemble the square of $\theta_F(E)$. We find this to be the case. The blue points in Fig. 4C show the total valley noise power versus the probe laser's energy. For comparison, red points show the square of the induced $\theta_F(E)$ shown in Fig. 4B, revealing a nearly identical spectral dependence. We emphasize that valley fluctuations can therefore be detected by FR using light tuned in energy well below the lowest absorption resonance in the WSe_2 monolayer, which further assures the nonperturbative nature of this noise-based approach, in which valley dynamics can be studied quantitatively under conditions of strict thermal equilibrium.

Lastly, Fig. 5 shows that valley noise is also detectable in a Fermi sea of resident electrons in monolayer TMDs. Here, $V_g = -2$ V, giving a small electron density $n \approx 1.2 \times 10^{12}/\text{cm}^2$. The probe laser is tuned to 1.686 eV or 7 meV below the negatively charged exciton (X^-) absorption. The measured noise spectrum is again Lorentzian, but its width Γ = 6.2 MHz is nearly an order of magnitude larger than the width of the hole noise spectrum in this same WSe_2 monolayer (cf. Fig. 1D). This indicates a much faster intrinsic relaxation time ($1/\pi\Gamma$ = 51 ns) for electrons as compared to holes, in agreement with the expectation that spin-valley locking is much weaker in the conduction bands than in the valence bands of monolayer TMDs (*29*). The inset of Fig. 5 shows a conventional TRFR study of this electron-doped monolayer, which closely corroborates the much faster relaxation of resident electrons, again confirming that (at least here) TRFR measurements are primarily sensitive to the valley polarization of resident electrons, and not dark exciton states.

DISCUSSION

These noise-based studies therefore demonstrate a promising new alternative approach for unambiguously probing the intrinsic valley dynamics of resident electrons and holes in monolayer TMD semiconductors. Spontaneous fluctuations of the valley polarization in strict thermal equilibrium are shown to encode the relevant time scales of valley relaxation and can be observed via sensitive FR noise spectroscopy without any external pumping or excitation. These proof-of-concept measurements reveal the long, monoexponential valley relaxation of holes and electrons in hBN-encapsulated WSe_2 monolayers. Moreover, this methodology validates the interpretation of traditional (perturbative) pump-probe spectroscopies that show long decays in doped TMD monolayers and resolves concerns about the role played by dark excitons, dark trions, and other long-lived excitations in valley relaxation measurements.

The fluctuation-based methods demonstrated here should be particularly suitable for future high-quality TMD monolayers and heterostructures for which the valley relaxation times are expected to

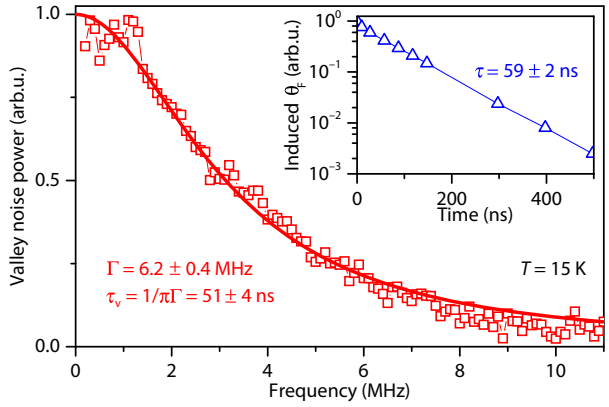

Fig. 5. The valley noise spectrum of electron-doped monolayer WSe_2. The spectrum shows Lorentzian line shape and much larger width Γ (indicating shorter valley relaxation time τ_v) as compared to the hole-doped regime (cf. Fig. 1D). The spectrum was measured at $V_g = -2$ V and $T = 15$ K using the off-WSe_2 background subtraction method. Inset: Electron valley relaxation measured independently by conventional (perturbative) TRFR, which corroborates the shorter τ_v.

be exceptionally long, such that features in the noise power spectra are narrow and large. We expect that under these conditions, the intrinsic valley relaxation time scales revealed by noise can be longer than the time scales accessible with perturbative methods, since any experimentally related perturbation (such as dark excitons or trapped states) may be stronger than the very weak interactions that lead to slow relaxation. This opens new opportunities for studies of valley physics in novel 2D semiconductors.

MATERIALS AND METHODS

Sample preparation

Flakes of hBN, WSe_2, and a few-layer graphene were mechanically exfoliated on Si/SiO_2 substrates. The van der Waals heterostructure assembly was performed using a polycarbonate dry transfer technique with a hot (110°C) pickup. The assembled heterostructure was then deposited onto prefabricated electrodes (50-nm Au on 5-nm Ti) made on a polished fused silica substrate to allow transmission of the probe laser beam through the sample.

Valley noise spectroscopy

Linearly polarized probe light from a tunable CW Ti:sapphire ring laser was focused through the sample. Valley fluctuations of resident carriers imparted small FR fluctuations $\delta\theta_F(t)$ on the transmitted light. These fluctuations were detected in an optical bridge consisting of a half-wave plate, polarization beamsplitter (Wollaston prism), and balanced photodiodes (Newport 1807). The resulting voltage signal $\delta V(t) \sim \delta\theta_F(t)$ was amplified and then digitized (AlazarTech ATS9462), and its power spectral density was continuously computed and signal averaged in real time using fast Fourier transform methods. Valley fluctuation noise constituted only a small fraction of the total measured noise power, which was dominated by uncorrelated broadband photon shot noise and electronic noise from the detectors. Thus, background subtraction was required to reveal the valley noise, as described in the Results section and in the Supplementary Materials.

Time-resolved Faraday rotation

To measure the valley polarization decay time of resident carriers using conventional (perturbative) pump-probe methods, we used TRFR. Ultrafast probe pulses were derived from a tunable pulsed Ti:sapphire laser. Its repetition rate was reduced by an acousto-optic pulse picker to achieve long (~10 μs) pulse separation. The pump pulses were produced by a 645-nm pulsed diode laser that was synchronized to the pulse picker, using an electronically controlled delay. The pump polarization was modulated between the right and left circular by a photoelastic modulator. Pumping with circularly polarized light injected valley-polarized electrons and holes, which induced a nonequilibrium valley polarization in the WSe_2. The decay of this valley polarization was measured using the FR induced on the time-delayed probe pulses, which was detected with balanced photodiodes and lock-in techniques.

Continuous-wave Faraday rotation

A steady-state nonequilibrium valley polarization of the resident carriers was induced using optical pumping with a CW 632.8-nm He:Ne pump laser. This nonequilibrium valley polarization was detected using a CW tunable Ti:sapphire probe laser (the same probe laser that is used, by itself, for the noise measurements). Polarization modulation of the pump beam and the detection of the induced FR on the probe beam were realized in the same manner as in the case of the TRFR measurement.

SUPPLEMENTARY MATERIALS

Supplementary material for this article is available at http://advances.sciencemag.org/cgi/content/full/5/3/eaau4899/DC1

Fig. S1. An example of the raw noise data.

Fig. S2. Valley noise spectra of resident holes at $B_x = 0$ and 0.35 T.

Fig. S3. Temperature and magnetic field dependence of the hole valley relaxation rate.

Fig. S4. Normalized transmission spectra of the WSe_2 monolayer in the hole- and electron-doped regime.

REFERENCES AND NOTES

1. Y. P. Shkolnikov, E. P. De Poortere, E. Tutuc, M. Shayegan, Valley splitting of AlAs two-dimensional electrons in a perpendicular magnetic field. *Phys. Rev. Lett.* **89**, 226805 (2002).
2. O. Gunawan, Y. P. Shkolnikov, K. Vakili, T. Gokmen, E. P. De Poortere, M. Shayegan, Valley susceptibility of an interacting two-dimensional electron system. *Phys. Rev. Lett.* **97**, 186404 (2006).
3. D. Xiao, W. Yao, Q. Niu, Valley-contrasting physics in graphene: Magnetic moment and topological transport. *Phys. Rev. Lett.* **99**, 236809 (2007).
4. A. Rycerz, J. Tworzydło, C. W. J. Beenakker, Valley filter and valley valve in graphene. *Nat. Phys.* **3**, 172–175 (2007).
5. D. Culcer, A. L. Saraiva, B. Koiller, X. Hu, S. Das Sarma, Valley-based noise-resistant quantum computation using Si quantum dots. *Phys. Rev. Lett.* **108**, 126804 (2012).
6. Z. Zhu, A. Collaudin, B. Fauqué, W. Kang, K. Behnia, Field-induced polarization of Dirac valleys in bismuth. *Nat. Phys.* **8**, 89–94 (2012).
7. J. Isberg, M. Gabrysch, J. Hammersberg, S. Majdi, K. K. Kovi, D. J. Twitchen, Generation, transport and detection of valley-polarized electrons in diamond. *Nat. Mater.* **12**, 760–764 (2013).
8. X. Xu, W. Yao, D. Xiao, T. F. Heinz, Spin and pseudospins in layered transition metal dichalcogenides. *Nat. Phys.* **10**, 343–350 (2014).
9. A. Kormányos, G. Burkard, M. Gmitra, J. Fabian, V. Zólyomi, N. D. Drummond, V. Fal'ko, k·p theory for two-dimensional transition metal dichalcogenide semiconductors. *2D Mater.* **2**, 022001 (2015).
10. J. R. Schaibley, H. Yu, G. Clark, P. Rivera, J. S. Ross, K. L. Seyler, W. Yao, X. Xu, Valleytronics in 2D materials. *Nat. Rev. Mater.* **1**, 16055 (2016).
11. W. Yao, D. Xiao, Q. Niu, Valley-dependent optoelectronics from inversion symmetry breaking. *Phys. Rev. B* **77**, 235406 (2008).
12. D. Xiao, G.-B. Liu, W. Feng, X. Xu, W. Yao, Coupled spin and valley physics in monolayers of MoS_2 and other group-VI dichalcogenides. *Phys. Rev. Lett.* **108**, 196802 (2012).
13. T. Cao, G. Wang, W. Han, H. Ye, C. Zhu, J. Shi, Q. Niu, P. Tan, E. Wang, B. Liu, J. Feng, Valley-selective circular dichroism of monolayer molybdenum disulphide. *Nat. Commun.* **3**, 887 (2012).

14. K. F. Mak, K. He, J. Shan, T. F. Heinz, Control of valley polarization in monolayer MoS_2 by optical helicity. *Nat. Nanotechnol.* **7**, 494–498 (2012).
15. Q. Wang, S. Ge, X. Li, J. Qiu, Y. Ji, J. Feng, D. Sun, Valley carrier dynamics in monolayer molybdenum disulfide from helicity-resolved ultrafast pump–probe spectroscopy. *ACS Nano* **7**, 11087–11093 (2013).
16. H. Ochoa, F. Finocchiaro, F. Guinea, V. I. Fal'ko, Spin-valley relaxation and quantum transport regimes in two-dimensional transition-metal dichalcogenides. *Phys. Rev. B* **90**, 235429 (2014).
17. G. Wang, L. Bouet, D. Lagarde, M. Vidal, A. Balocchi, T. Amand, X. Marie, B. Urbaszek, Valley dynamics probed through charged and neutral exciton emission in monolayer WSe_2. *Phys. Rev. B* **90**, 075413 (2014).
18. T. Yu, M. W. Wu, Valley depolarization due to intervalley and intravalley electron-hole exchange interactions in monolayer MoS_2. *Phys. Rev. B* **89**, 205303 (2014).
19. C. Mai, A. Barrette, Y. Yu, Y. G. Semenov, K. W. Kim, L. Cao, K. Gundogdu, Many-body effects in valleytronics: Direct measurement of valley lifetimes in single-layer MoS_2. *Nano Lett.* **14**, 202–206 (2014).
20. N. Kumar, J. He, D. He, Y. Wang, H. Zhao, Valley and spin dynamics in $MoSe_2$ two-dimensional crystals. *Nanoscale* **6**, 12690–12695 (2014).
21. A. Singh, K. Tran, M. Kolarczik, J. Seifert, Y. Wang, K. Hao, D. Pleskot, N. M. Gabor, S. Helmrich, N. Owschimikow, U. Woggon, X. Li, Long-lived valley polarization of intravalley trions in monolayer WSe_2. *Phys. Rev. Lett.* **117**, 257402 (2016).
22. Y. Song, H. Dery, Transport theory of monolayer transition-metal dichalcogenides through symmetry. *Phys. Rev. Lett.* **111**, 026601 (2013).
23. W.-T. Hsu, Y.-L. Chen, C.-H. Chen, P.-S. Liu, T.-H. Hou, L.-J. Li, W.-H. Chang, Optically initialized robust valley-polarized holes in monolayer WSe_2. *Nat. Commun.* **6**, 8963 (2015).
24. L. Yang, N. A. Sinitsyn, W. Chen, J. Yuan, J. Zhang, J. Lou, S. A. Crooker, Long-lived nanosecond spin relaxation and spin coherence of electrons in monolayer MoS_2 and WS_2. *Nat. Phys.* **11**, 830 (2015).
25. X. Song, S. Xie, K. Kang, J. Park, V. Sih, Long-lived hole spin/valley polarization probed by Kerr rotation in monolayer WSe_2. *Nano Lett.* **16**, 5010–5014 (2016).
26. T. Yan, S. Yang, D. Li, X. Cui, Long valley relaxation time of free carriers in monolayer WSe_2. *Phys. Rev. B* **95**, 241406 (2017).
27. E. J. McCormick, M. J. Newburger, Y. K. Luo, K. M. McCreary, S. Singh, I. B. Martin, E. J. Cichewicz Jr., B. T. Jonker, R. K. Kawakami, Imaging spin dynamics in monolayer WS_2 by time-resolved Kerr rotation microscopy. *2D Mater.* **5**, 011010 (2018).
28. J. Kim, C. Jin, B. Chen, H. Cai, T. Zhao, P. Lee, S. Kahn, K. Watanabe, T. Taniguchi, S. Tongay, M. F. Crommie, F. Wang, Observation of ultralong valley lifetime in WSe_2/MoS_2 heterostructures. *Sci. Adv.* **3**, e1700518 (2017).
29. P. Dey, L. Yang, C. Robert, G. Wang, B. Urbaszek, X. Marie, S. A. Crooker, Gate-controlled spin-valley locking of resident carriers in WSe_2 monolayers. *Phys. Rev. Lett.* **119**, 137401 (2017).
30. M. R. Molas, C. Faugeras, A. O. Slobodeniuk, K. Nogajewski, M. Bartos, D. M. Basko, M. Potemski, Brightening of dark excitons in monolayers of semiconducting transition metal dichalcogenides. *2D Mater.* **4**, 021003 (2017).
31. Y. Zhou, G. Scuri, D. S. Wild, A. A. High, A. Dibos, L. A. Jauregui, C. Shu, K. De Greve, K. Pistunova, A. Y. Joe, T. Taniguchi, K. Watanabe, P. Kim, M. D. Lukin, H. Park, Probing dark excitons in atomically thin semiconductors via near-field coupling to surface plasmon polaritons. *Nat. Nanotechnol.* **12**, 856–860 (2017).
32. X.-X. Zhang, T. Cao, Z. Lu, Y.-C. Lin, F. Zhang, Y. Wang, Z. Li, J. C. Hone, J. A. Robinson, D. Smirnov, S. G. Louie, T. F. Heinz, Magnetic brightening and control of dark excitons in monolayer WSe_2. *Nat. Nanotechnol.* **12**, 883–888 (2017).
33. G. Wang, C. Robert, M. M. Glazov, F. Cadiz, E. Courtade, T. Amand, D. Lagarde, T. Taniguchi, K. Watanabe, B. Urbaszek, X. Marie, In-plane propagation of light in transition metal dichalcogenide monolayers: Optical selection rules. *Phys. Rev. Lett.* **119**, 047401 (2017).
34. G. Plechinger, P. Nagler, A. Arora, R. Schmidt, A. Chernikov, A. G. del Águila, P. C. M. Christianen, R. Bratschitsch, C. Schüller, T. Korn, Trion fine structure and coupled spin-valley dynamics in monolayer tungsten disulfide. *Nat. Commun.* **7**, 12715 (2016).
35. F. Volmer, S. Pissinger, M. Ersfeld, S. Kuhlen, C. Stampfer, B. Beschoten, Intervalley dark trion states with spin lifetimes of 150 ns in WSe_2. *Phys. Rev. B* **95**, 235408 (2017).
36. R. Kubo, The fluctuation-dissipation theorem. *Rep. Prog. Phys.* **29**, 255–284 (1966).
37. S. A. Crooker, D. G. Rickel, A. V. Balatsky, D. L. Smith, Spectroscopy of spontaneous spin noise as a probe of spin dynamics and magnetic resonance. *Nature* **431**, 49–52 (2004).
38. V. S. Zapasskii, Spin-noise spectroscopy: From proof of principle to applications. *Adv. Opt. Photon.* **5**, 131–168 (2013).
39. M. Oestreich, M. Römer, R. J. Haug, D. Hägele, Spin noise spectroscopy in GaAs. *Phys. Rev. Lett.* **95**, 216603 (2005).
40. S. A. Crooker, L. Cheng, D. L. Smith, Spin noise of conduction electrons in *n*-type bulk GaAs. *Phys. Rev. B* **79**, 035208 (2009).
41. V. S. Zapasskii, A. Greilich, S. A. Crooker, Y. Li, G. G. Kozlov, D. R. Yakovlev, D. Reuter, A. D. Wieck, M. Bayer, Optical spectroscopy of spin noise. *Phys. Rev. Lett.* **110**, 176601 (2013).

Acknowledgments: We thank Ł. Kłopotowski for helpful discussions and A. Balk for assistance with the digitizer. **Funding:** We acknowledge support from the Los Alamos LDRD program. Work at the NHMFL was supported by NSF DMR-1644779, the State of Florida, and the U.S. DOE. Work at the University of Washington was supported by the DOE Basic Energy Sciences, Materials Sciences and Engineering Division (DE-SC0018171). **Author contributions:** S.A.C. and X.X. conceived the research. N.P.W. fabricated the samples. M.G. and P.D. performed the optical measurements. M.G. performed the data analysis. All authors discussed the results. M.G. and S.A.C. wrote the manuscript in consultation with all the other authors. **Competing interests:** The authors declare that they have no competing interests. **Data and materials availability:** All data needed to evaluate the conclusions in the paper are present in the paper and/or the Supplementary Materials. Additional data related to this paper may be requested from the authors.

Submitted 15 June 2018
Accepted 14 January 2019
Published 1 March 2019
10.1126/sciadv.aau4899

Citation: M. Goryca, N. P. Wilson, P. Dey, X. Xu, S. A. Crooker, Detection of thermodynamic "valley noise" in monolayer semiconductors: Access to intrinsic valley relaxation time scales. *Sci. Adv.* **5**, eaau4899 (2019).

ScienceAdvances

Detection of thermodynamic "valley noise" in monolayer semiconductors: Access to intrinsic valley relaxation time scales

M. Goryca, N. P. Wilson, P. Dey, X. Xu and S. A. Crooker

Sci Adv **5** (3), eaau4899.
DOI: 10.1126/sciadv.aau4899